Tikrit Journal of Engineering Sciences (2022) 29 (4): 27-39
DOI: http://doi.org/10.25130/tjes.29.4.4

IRAQI Academic Scientific Journals

ISSN: 1813-162X (Print); 2312-7589 (Online)

Tikrit Journal of Engineering Sciences

available online at: http://www.tj-es.com

TJES Tikrit Journal of Engineering Sciences

College of Engineering

Shear Behavior of Hollow Ferrocement Beam Reinforced by Steel and Fiberglass Meshes

*Qutaiba Najm Abdullah * [1, 2], Aziz Ibrahim Abdulla[2, 3, 4], Mustafa Al-Mashaykhi[5]*

1 *Civil Eng, Dept., Al-Qalam University College.*
2 *Civil Eng. Dept., College of Engineering, Tikrit University, Tikrit, Iraq.*
3 *Civil Eng. Dept., College of Engineering, Al-Ahliyya Amman University, Jordan.*
4 *Civil Eng. Dept., College of Engineering, University Malaya, Malaysia.*
5 *Swinburne University of Technology, Australia.*

Keywords:

Ductility; Fiberglass mesh; Hollow-ferrocement beam; Self-compacted mortar; Shear behavior; Steel wire mesh; Toughness; Ultimate load

ARTICLE INFO

Article history:

Received	05 Nov. 2022
Accepted	16 Dec. 2022
Available online	20 Dec. 2022

Citation: Abdullah QN, Abdulla AI, Al-Mashaykhi M. Shear Behavior of Hollow Ferrocement Beam Reinforced by Steel and Fiberglass Meshes. Tikrit Journal of Engineering Sciences 2022; 29(4): 27-39.
http://doi.org/10.25130/tjes.29.4.4

Corresponding author:

Qutaiba Najm Abdullah, E-mail: qutaiba.najm@gmail.com, Civil Department, College of Engineering, Tikrit University, Tikrit, Iraq.

ABSTRACT

The purpose of this study is to investigate the shear behavior of hollow ferrocement beams of self-compacting mortar reinforced with various types of metallic (steel wire mesh) and non-metallic (fiberglass mesh) reinforcement. The experimental program consists of casting eight ferrocement beams with dimensions of 150×225×2000 mm, 50 mm of ferrocement thickness, and a polystyrene cork core of 50×125 mm. The studied parameters were the shear reinforcement type and the number of wire mesh layers. The results showed that the ultimate load of the beams reinforced with several layers of the fiberglass mesh (1, 2, and 3) was decreased by (3.27%, 16.52%, and 9.38%), respectively, compared to the beams reinforced with layers of steel wire mesh (1, 2, and 3). The ultimate load of these beams increased by (33.71%, 73.28%, and 122.11%) respectively, compared to beams without shear reinforcement. Also, the ultimate load of the beams reinforced with layers of welded wire mesh was increased by (38.23%, 107.56%, and 145.09%), respectively, compared to beams without shear reinforcement. The ductility and toughness of the beams reinforced with several layers of the fiberglass mesh (1, 2, and 3) were decreased by (1.68%, 2.11%, 2.68%) and (29.39%, 25.91%, 16.06%), respectively, compared to beams reinforced with several layers of steel wire mesh (1, 2, and 3). The crack propagation was reduced, and its number and width decreased using steel wire mesh and fiberglass wire mesh instead of stirrups, especially in beams with two and three layers of wire mesh. The results also showed that the use of glass fiber or welded wire mesh in the reinforcement of hollow beams instead of steel stirrups significantly affected the failure load, deflections, crack patterns, and shear stresses, despite the clear preference for beams reinforced with steel wire mesh.

تصرف القص للعتبات الفيروسمنتية المجوفة المسلحة بشبكات حديدية وشبكات من الألياف الزجاجية

قتيبة نجم عبدالله قسم الهندسة المدنية / كلية القلم الجامعة / العراق.
قسم الهندسة المدنية / كلية الهندسة / جامعة تكريت / تكريت - العراق.
عزيز ابراهيم عبدالله قسم الهندسة المدنية / كلية الهندسة / جامعة تكريت / تكريت - العراق.
قسم الهندسة المدنية / كلية الهندسة / جامعة عمان الاهلية / الاردن.
قسم الهندسة المدنية / كلية الهندسة / جامعة ملايا / ماليزيا.
مصطفى المشايخي جامعة سومبيرن للتكنلولوجيا / استراليا.

الخلاصة

الغرض من هذه الدراسة هو التحقق من سلوك القص للعتبات الفيروسمنية المجوفة المصنوعة من ملاط أسمنتي ذاتي الرص مسلحة بأنواع مختلفة من التعزيزات المعدنية (شبكة سلكية حديدية) وغير معدنية (شبكة الألياف الزجاجية). يتكون البرنامج التجريبي من صب ثمانية عتبات فيروسمنية بأبعاد 150 × 225 × 2000 مم وبسمك 50 مم من الفيروسمنت ولب من الفلين البوليسترين 50 × 125 مم. كانت متغيرات الدراسة تشمل نوع التسليح للقص وعدد طبقات الشبكات السلكية (واحد، اثنان، ثلاثة). أظهرت النتائج أن الحمل الاقصى للعتبات المسلحة بعدة طبقات من شبكة الألياف الزجاجية (واحد، اثنان، ثلاث) انخفض بنسبة (3.27٪، 16.52٪، 9.38٪) على التوالي، مقارنة بالعتبات المسلحة بطبقات من شبكة أسلاك الحديدية (واحد، اثنان وثلاثة). الا ان الحمل الاقصى لهذه العتبات ازداد بنسبة (33.71٪، 73.28٪، 122.11٪) على التوالي، مقارنة بالعتبات غير المسلحة للقص. كما ان الحمل الاقصى للعتبات المسلحة بطبقات من الشبكات السلكية الحديدية ازداد بنسبة (38.23٪، 107.56٪، 145.09٪) على التوالي، مقارنة بالعتبات غير المسلحة للقص فقط بالمونة الأسمنتية. طاقة الليونة والمتانة للعتبات المسلحة بعدة طبقات من شبكة الألياف الزجاجية (واحد، اثنان، ثلاثة) انخفضت بنسبة (1.68٪، 2.11٪، 2.68٪) و (29.39٪، 25.91٪، 16.06٪) على التوالي، مقارنة بالعتبات المسلحة بعدة طبقات من شبكة أسلاك الفولاذ (واحد، اثنان، ثلاثة). أدى استخدام الشبكات الفولاذية والزجاجية بدلاً من الركائب إلى تقليل انتشار الشقوق وعدد الشقوق وعرض الشقوق، خاصة في الحزم باستخدام طبقتين وثلاث طبقات من الشبكات. كما أظهرت النتائج أن استخدام الألياف الزجاجية أو شبكة الأسلاك الحديدية في تقوية الكمرات المجوفة بدلاً من الركائب الفولاذية له تأثير جيد على الحمل الاقصى والانحرافات وأنماط الشقوق وإجهادات القص، على الرغم من افضلية العتبات المقواة بشبكات حديدية بشكل واضح.

الكلمات الدالة: شبكة الالياف الزجاج، شبكة اسلاك حديدية، عتبة فيروسمنية مجوفة، ملاط ذاتي الرص، تصرف القص، الحمل الاقصى، المطيلية، المتانة.

1. INTRODUCTION

One of the significant forms of reinforced concrete is known as ferrocement. It is a reinforced mortar matrix with numerous layers of meshes or small bars saturated in cement mortar. As one type of ferrocement, mesh layers are welded wire meshes, woven wire meshes, and expanded wire meshes. Ferrocement has been utilized for numerous applications, including boats, dwellings, bus stations, bridges, irrigation, retaining walls, artwork, and buildings [1,2]. Additionally, for the restoration of reinforced concrete structures, it is a great substitute for reinforcing elements [3–5]. Corrosion of steel reinforcement in reinforced concrete structures is a significant problem that degrades the material when it interacts with the environment [6,7]. It affects the durability of the concrete construction. To reinforce concrete constructions, engineers sought materials that could survive adverse environmental conditions. Glass Fiber Reinforced Polymer (GFRP) rebar has high corrosion resistance. Also, it has been developed as a potential substitute for conventional steel because it prevents concrete from weakening. A few of its benefits are high tensile strength, high rigidity-to-weight ratio, protection from corrosion and chemical attack, low weight, regulated thermal expansion, and electromagnetic neutrality. Fiber-reinforced plastic (FRP) bars have a linear elastic behavior up until failure (brittleness), which affects the ductility of concrete elements. Moreover, the failure processes of FRP-reinforced concrete (FRP-RC) members depend on the reinforcing level. Most design specifications and guidelines advise over reinforcing FRP-reinforced parts to ensure plastic deformation of the concrete and enhance the ductility of the structure [8]. Fiberglass wire mesh is one type of fiber-reinforced polymer FRP. It is also more resistant to corrosion, has a high tensile strength, and does not get magnetized. It has many applications in buildings, such as insulating the inside and outside of walls, keeping out the weather, and preventing cracks [9,10]. Shaaban [11] studied the possibility of ferrocement's usage as a formwork to enhance the structural behavior of bent concrete beams. It was found that employing wings made of the same material and expanded wire fabric as permanent templates increased the maximum load by 20% and decreased crack widths by about 35%. Qu et al. [12] and Li et al. [13] studied the bending behavior of GFRP-reinforced concrete beams and steel bars, respectively. A GFRP-reinforced beam has better flexural behavior than steel in load-carrying capacity and toughness, but it has lower ductility and wide crack width. Shaheen

et al. [14] investigated the effectiveness of the channel beam under two-point loads up to failure. The beams were constructed from welded, expanded, and fiberglass meshes. They concluded that the initial crack loads, service loads, ultimate loads, and toughness of ferrocement reinforcing using welded wire meshes were greater than those reinforced with glass or expanded meshes. Erfan and El-Sayed [15,16] investigated the shear strength of box beams reinforced by expanded wire mesh, welded meshes, polyethylene meshes, and fiberglass meshes. The study's findings show that using these meshes rather than steel stirrups to reinforce box sections significantly influenced ultimate loads, deflections, cracks growth, and shear strength. They were also lighter than steel stirrups. When comparing the shear resistance of various wire mesh materials, welded and expanded meshes out performed polyethylene and fiberglass meshes. Abdallah et al. [17] conducted an experimental and theoretical study of ferrocement panels reinforced with expanded and welded wire mesh. The theoretical analysis was performed by Ansys 14.5. Experimental results showed that using expanded steel mesh as reinforcing materials showed lower deflection and greater flexural strength than panels reinforced with welded wire mesh. The analytical results showed good agreement with the results of the experiment. El-Sayed [18] investigated the ferrocement columns' performance, with sizes of (150 × 150 × 1600) mm that were reinforced by metallic meshes (expanded and welded wire mesh) besides non-metallic materials (polyethylene and glass mesh fibers). ANSYS2019-R1 was used to conduct an experiment plan and make a finite element prototype. The final loads and energy absorbed by metal mesh ferrocement columns were higher than those of non-metal mesh ferrocement columns. There was concordance between the analyzed and experimental results. Numerous researchers have recently, such as Khalil et al. [19], Lee et al. [20,21], Wariyatno et al. [22], and Rajeshwaran et al. [23], analyzed the performance of conventional hollow concrete members. In contrast, fewer investigations, including Abdulla and Hadi [24] and Chkheiwer et al. [25], conducted studies to test the structural behavior of hollow core metallic reinforcing elements. Therefore, the objective of this research is to investigate and compare the shear strength of box ferrocement beams with self-compacted mortar reinforced using fiberglass wire meshes to that of box ferrocement beams reinforced by ordinary wire meshes. Also, the present study aims to evaluate the resistance of the fiberglass meshes to the shear forces. This study used full-size samples to investigate the real behavior of hollow beams.

2. EXPERIMENTAL PROGRAM

2.1. Materials

- Cement (C): The cement used in the present work was Iraqi, locally called Al-Mas. It conforms with the Iraqi standard [26]. Table.1 shows the chemical properties of the used cement. Table.2 shows the physical properties of the used cement.

Table.1 Chemical properties of cement.

Composition	Cement (%)
CaO	63.34
SiO_2	21.09
Al_2O_3	5.09
Fe_2O_3	3.03
MgO	1.91
SO_3	2.28
Loss on ignition	1.46
Insoluble material	0.27
Lime saturation factor	0.92
C_3A	8.36
C_3S	52.46
C_2S	21.08
C_4AF	9.23

Table.2 Physical properties of cement.

Physical property	Results	Limit of I.Q.S. No. (5/1984,2/2010)
Fineness (m^2/Kg)	361	Not less than 230 m^2/Kg
Initial Setting (min.)	160	Not less than 45min.
Final Setting (min.)	290	Not more than 600min.
3 days age (N/mm^2)	19.3	Not less than 15
7 days age (N/mm^2)	23.7	Not less than 23

- Sand (S): River sand was used as the fine aggregate in this study. It complies with Iraqi standards [27]. Table.3 shows the physical and chemical properties of the sand. It has a fineness modulus of three. Table.4 shows the particle size distribution of the used sand.

Table.3 Physical and chemical properties of the used sand.

Properties	Results
Specific gravity	2.44
Absorption %	2.05
Dry loose unit weight, kg/m^3	1750
Sulfate content (as SO_3), %	0.3
Material finer than 0.075 mm% sieve	2.3

Table.4 Sieve analysis of sand.

Sieve size	Cumulative passing %	Limit of I.Q.S. No.(45/1984,2/2010)
(3/8-in.) 10-mm	100	100
(No. 4) 4.75-mm	95.5	90 to 100
(No. 8) 2.36-mm	77	75 to 100
(No. 16) 1.18-mm	60.3	55 to 90
(No. 30) 600-µm	47.16	35 to 59
(No. 50) 300-µm	21.76	8 to 30
(No. 100) 150-µm	4.26	0 to 10

- Limestone Powder (LSP): It is a locally available material with a density of 1403 kg/m^3 and a specific gravity of 2.69. It was used in the mixture as filler after carrying out sieve analysis, as shown in Table.5. Limestone powder has a vital role in improving the flowability when producing self-compacting mortar mixtures [28].

Table.5 Sieve analysis of limestone powder.

Sieve size	Cumulative passing %
(No. 50) 300-µm	100
(No. 100) 150-µm	87.53
(No. 200) 75-µm	73.45

- Water (W): Potable water was used in the design of the self-compacting mortar mixture.

- Superplasticizer (SP): The MegaFlow 110 type F, as a high-range water-reducing admixture, was used in this work. It conforms to ASTM C494 [29] and has a specific gravity of 1.08 at 25°C. The recommended dosage range is 0.5–2% of mass cementitious materials.

- Reinforcing steel bars: In this study, two diameters of steel rebars were used. Φ12 mm rebars with a yield strength of 620 MPa were utilized for longitudinal reinforcing, whereas Φ6 mm rebars with a yield strength of 510 MPa were employed for stirrups on transversely reinforced beams. The reinforcing bars' physical properties were examined by ASTM A615M-16 [30]. Table.6 shows the properties of steel bars. Fig.1 shows the testing bars.

- Reinforcement mesh

▪ Steel wire mesh: A square welded wire mesh was used in this work, available in local markets, with a diameter of 1 mm, and a grid size of 10×10 mm. The properties of the wire mesh were tested by ASTM A1064M-18 [31], as shown in Fig.2. The test results have shown that the wire had a yield strength of 287.5 MPa and the ultimate strength of 357.69 MPa, while the weight of one square meter was 0.765kg/m². The test results are shown in Table.7.

▪ Fiberglass mesh: A special fiberglass mesh was used in this study that was unavailable in local markets. It has an opening size of 10×10 mm and 1.2 mm thickness. The weight of mesh per square meter was 0.45 kg/m². The characteristics of these meshes were tested in conformance to ASTM A1064M-18 [31], as shown in Fig.2. The results of the tests are shown in Table.7.

Table.6 Characteristics of the steel bars.

Rebars	Diameter (mm)	Weight (g/m)	Yield strength (MPa)	Ultimate Strength (MPa)
Steel	12	847	620	725
Steel	6	198	510	538.8

Fig.1 Test steel bars.

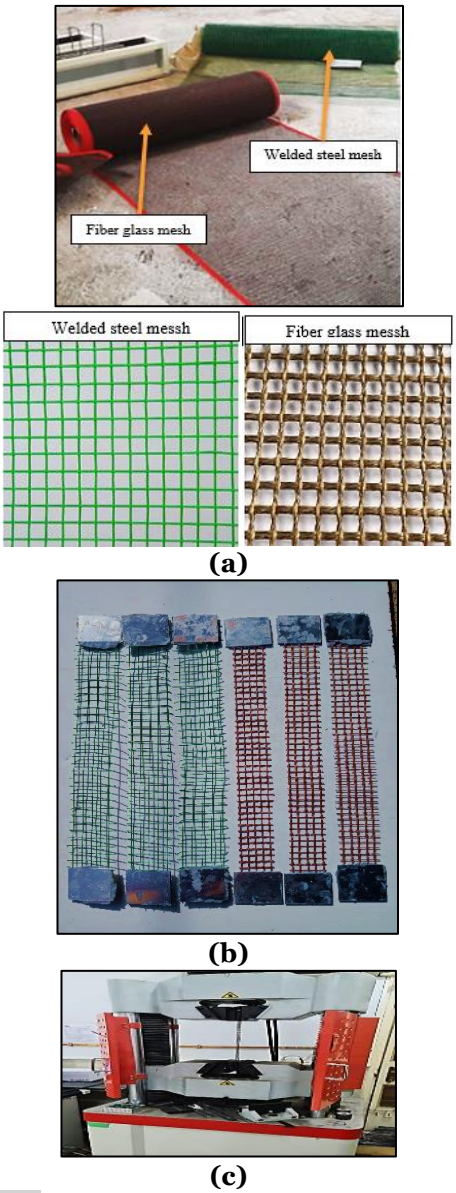

Fig. 2 (a)Welded wire mesh and glass mesh, (b) Samples for testing and (c) Testing of tensile strength.

Table.7 Characteristics of the wire meshes.

Mesh type	Mesh size (mm)	Diameter (mm)	Thickness (mm)	Weight (g/m²)	Warp yield stress (MPa)	Weft yield stress (MPa)	Warp ultimate stress (MPa)	Weft ultimate stress (MPa)	Young's modulus (MPa)
Welded steel mesh	10×10	1	---------	765	286.8	287.5	355.41	357.69	130363
Fiberglass mesh	10×10	---------	1.2	450	---------	---------	352.86	302.89	12693

2.2. Mortar matrix

In this study, all the studied beams were cast in a self-compacted mortar. To obtain the mixture of self-compacted, several experimental mixes were conducted. All the tests of self-compacted were conducted on fresh mortar according to EFNARC-05 [32] and several researchers, Libre et al. [33], Mehdipour et al. [34], Mahdikhani et al. [35], and Yaseri et al. [36]. The tests consisted of a mini-slump test, mini V-funnel test, mini J-ring test, and mini-column segregation, as depicted in Fig.3. The mix ratios of the self-compacting mortar were cement to sand 1:2, water to cement (W/C) 0.35, limestone powder 15% of the cement weight, and superplasticizer of 1.35% of the weight of cement. Table.8 shows the components of self-compacting mortar. Table.9 shows the new characteristics of self-compacting mortar mixtures. The hardened characteristics include a test of compressive strength using cubes (50×50×50) mm was tested at 28 days according to ASTM C109 [37]. The modulus of rupture by casting prisms with dimensions of (40×40×160) mm was tested at the age of 28 days according to ASTM C348 [38]. Also, the splitting tensile strength of cement mortar with 100 mm in diameter and 200 mm in length dimensions was tested at the age of 28 days according to ASTM C496 [39]. Table.10 shows the hardened properties of self-compacting mortar.

Fig. 3 Testing of the self-compacting mixture.

Table.8 Proportions of self-compacting mortar mixture.

Mixture	LSP	W/C	Cement (kg/m³)	Limestone powder (kg/m³)	Water (kg/m³)	Sand (kg/m³)	SP (kg/m³)
Self-compacting mortar	15%	0.35	596.4	89.46	208.74	1192.8	9.26

Table.9 The rheological properties of fresh self-compacting mortar mixture.

Type test	Result	Limits	According to
Mini slump flow (mm)	253	250±10	(EFNARC-2005)[32]
Mini J – ring (mm)	251	----------	----------
Difference between mini-slump and mini-J ring spread (mm)	2	≤ 15	(Mahdikhani et al., 2015)[35]
Difference between H in - H out mini-J ring test (mm)	3	≤ 10	(Yaseri et al., 2018)[36]
Mini V-funnel flow time (sec)	10.1	9±2	(EFNARC-2005) [32]
Mini V-funnel at T_5 minutes (sec)	12.7	----------	----------
Time increase V-funnel at T_5 minutes (sec)	2.6	≤ +3	(EFNARC-2005) [32]
Mini column segregation S (%)	6.31	≤ 30	(Libre et al., 2010[33]; Mehdipour, 2013[34]; Mahdikhani et al., 2015 [35])

Table.10 Hardened properties of self-compacting mortar.

Mixture	Compressive Strength (MPa)		Splitting strength (MPa)	Flexural Strength (MPa)
	7 Days	28 Days	28 Days	28 Day
Self-compacting mortar	40.58	47.03	7.34	9.78

2.3. Description of beams

To study the behavior of steel wire mesh and fiberglass mesh for shear forces, eight different reinforced hollow ferrocement beams of self-compacting mortar were made. The dimensions of the hollow beams were 150 × 225 × 2000 mm, and a span of 1800 mm with a hollow core of 125 × 50 mm of polystyrene cork and 50 mm thickness of ferrocement, as shown in Fig. 4. All beams were designed to be tested under a two-

point-load with a distance of 600 mm. The shear span (a) was 600 mm, and the effective depth (d) was 200 mm. All beams were designed with a constant ratio of shear span to effective depth (a/d) equals three. All beams were reinforced 4Φ12 at the bottom and 2Φ8 at the top. Two beams were designed as reference beams. One of the beams (BHNS) was designed without any stirrups or wire mesh to resist shear forces, meaning that it only fails to resist this self-compacting mortar to shear forces. The second beam (BHWS) was designed by reinforcing it only with steel stirrups to resist shear forces. The stirrups for this beam were Φ6@125mm. The parameters of the remaining six beams were changed to the number of wire mesh layers and wire mesh type. Three beams (BHWS1, BHWS2, and BHWS3) were only reinforced with one, two, and three layers of welded wire mesh. Also, the other three beams (BHWG1, BHWG2, and BHWG3) were only reinforced with one, two, and three layers of fiberglass mesh. Table.11 and Fig. 5 show the details of the beam's reinforcement.

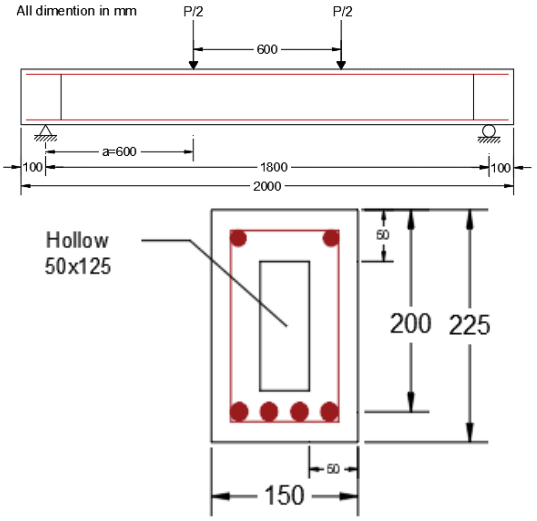

Fig. 4 Beams dimensions.

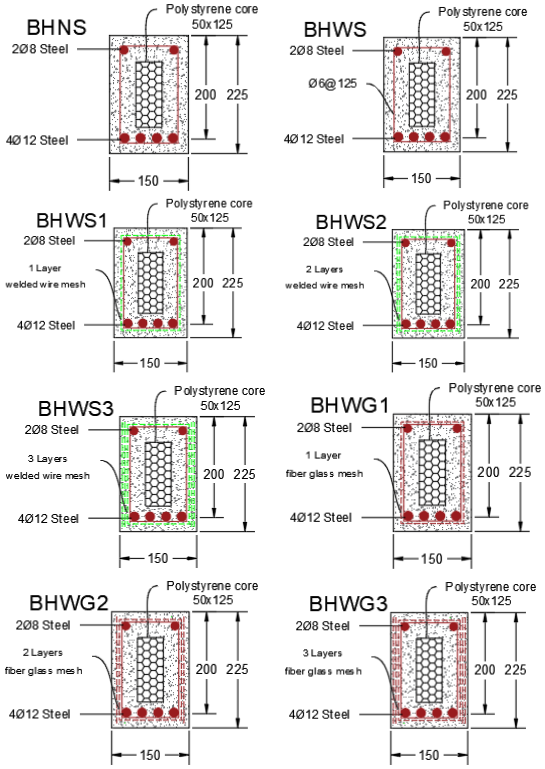

Fig. 5 Details of the reinforcing of shear in beams. All dimensions in mm.

2.4. Ferrocement beams casting

For casting ferrocement beams, the necessary materials were prepared, and the mixture required for casting (self-compacting mortar) was designed. Hollow molds were created with an opening on both sides, and a core of polystyrene cork was used to fill this hollow. The beams were cast by an electric concrete mixer. The beams were treated for 28 days using burlap bags and sand [40]. After this time, the beams were ready for testing. Fig.6 shows the procedures of reinforcement and casting.

Table.11 Details of beams reinforcement.

Model	Top reinforcing	bottom reinforcing	Steel stirrups	No. of wire mesh		Shear reinforcement ratio %	Type of shear reinforcement
				flange	web		
BHNS	2Φ8	4Φ12	----------	0	0	0	Mortar only
BHWS	2Φ8	4Φ12	Φ6@125mm	0	0	0.301	Steel stirrups
BHWS1	2Φ8	4Φ12	----------	1	1	0.104	Steel wire mesh
BHWS2	2Φ8	4Φ12	----------	1	2	0.209	
BHWS3	2Φ8	4Φ12	----------	1	3	0.314	
BHWG1	2Φ8	4Φ12	----------	1	1	0.119	Fiberglass mesh
BHWG2	2Φ8	4Φ12	----------	1	2	0.239	
BHWG3	2Φ8	4Φ12	----------	1	3	0.359	

Beams reinforcement.

The casting of the beams using self-compacting mortar.

Beams curing.

Fig. 6 Beams' reinforcement and casting with GFRP mesh and self-compacting mortar.

2.5. Beams test

All specimens were subjected to the two-point load test with a distance of 600 mm. The shear span (a) was 600 mm, and the effective depth (d) was 200 mm. The ferrocement beams were designed with a constant ratio of shear span to effective depth (a/d) equals three. Each beam in the machine was installed on simple supports with a clear span of 1800 mm. The hollow ferrocement beams were tested using a hydraulic machine with a capacity of 2000 kN. To measure the deflection, a linear variable displacement transducer (LVDT) was positioned in the center of the beam, as shown in Fig. 7. All ferrocement beams were pigment by white color for cracks to be easily observed using a micro crack width camera calibrated to 0.005 mm. The displacement rate on beams was 1.5 mm/min. The deflection and load of the beams were automatically recorded by a computer data logger device. Crack patterns were examined with every loading phase. The positions and development of cracks were indicated on the side surfaces of the shear beams [41,42]. Fig. 8 shows the shear beam testing.

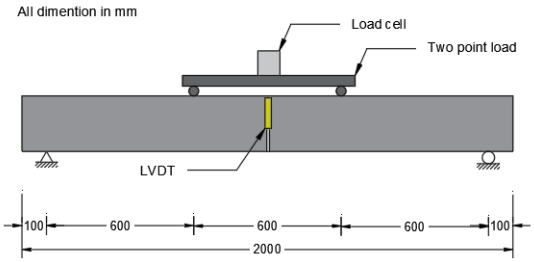

Fig. 7 Test diagram for shear beams.

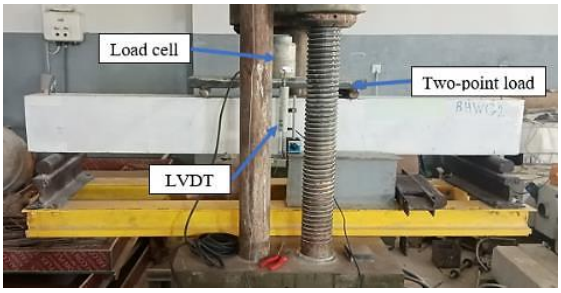

(a) Beam test.

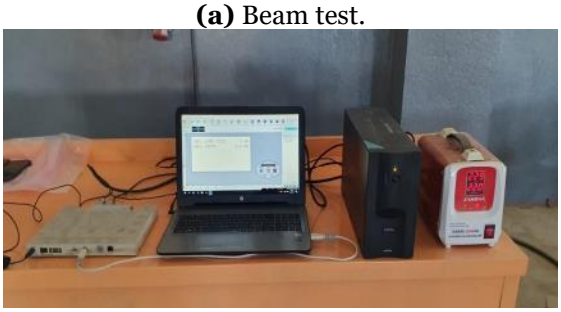

(b) Data logger to monitor the load and deflection.

(c) Micro crack width (camera system).

Fig. 8 Testing of the shear ferrocement.

3. RESULTS AND DISCUSSION

The present study examined first crack loads, ultimate loads, deflections at the first crack loads, deflections at the ultimate loads, ductility, cracks' patterns, and failure mechanism (see Fig. 9). A load-deflection curve was also found for the examined beams. Fig.10 shows the relationships of the load-deflection of the investigated beam. Table.12 shows the testing results of shear ferrocement beams reinforced by glass mesh and steel mesh.

Fig. 9 Failure of shear ferrocement beam reinforced using steel and glass mesh.

3.1. Ultimate loads and load-deflection curves

Load and displacement relations of the studied beams are shown in Fig.10. This figure describes the relationships between hollow beams reinforced using the mesh of fiberglass and those reinforced using welded steel wire mesh, as well as a comparison between the two reinforcements. Table.12 shows the shear beam results. The ultimate loads of beams reinforced with glass mesh (BHWG1, BHWG2, BHWG3) were decreased by (3.27%, 16.52%, and 9.38%), respectively, compared with beams reinforced using layers of steel mesh (BHWS1, BHWS2, BHWS3). This decrease in load was due to differences in the tensile strength, which was more significant in the welded wire mesh. However, the ultimate load of these beams was increased by (33.71%, 73.28%, and 122.11%), respectively, compared to the beams that were un-reinforced to shear (BHNS). Also, the ultimate load of beams reinforced by layers of welded mesh (BHWS1, BHWS2, BHWS3) was increased by about (38.23%, 107.56%, and 145.09%), respectively, compared to the beams that were un-reinforced to shear (BHNS). This loads increase was due to reinforcing these beams with a fiberglass or steel mesh [43]. Steel wire mesh layers were more load resistant than fiberglass mesh layers. The loads were increased by 50.16 % and 77.31, on the beams reinforced with 2 and 3 layers of metal meshes (BHWS2, BHWS3) %, respectively, when with the beam (BHWS1). The loads were enhanced by 29.59% and 66.11%, respectively, in the beams reinforced using two and three layers of glass mesh (BHWG2, BHWG3) compared with the beam (BHWG1). This conclusion is consistent with what has been reported by Erfan and El-Sayed [15,16]. All of the ferrocement reinforced using steel mesh or glass mesh (BHWS1, BHWS2, BHWS3, BHWG1, BHWG2, BHWG3) were reduced in the ultimate loads by (49.36%, 23.96%, 10.21%, 51.02%, 36.52%, 18.63%), respectively, compared to beam BHWS. This reduction in load was because of reinforced this beam BHWS, which was reinforced with steel bars, not any mesh. Therefore, the area of shear reinforcement was more significant than the mesh. For this reason, the ultimate load on beam BHWS was more significant than all other beams. The maximum deflection of all ferrocement reinforced using glass mesh was slightly less than that of ferrocement reinforced using steel mesh, as shown in Table.12. All of the beams reinforced using glass mesh had lower first crack loads than the beams reinforced by steel mesh. The GFRP beams' first crack deflection was close to that of steel beams. In addition, the load-deflection relationships of ferrocement beams in all figures showed that the beams reinforced by steel or glass mesh exhibited a linear relationship to the ultimate point load. The shear behavior was linear in the concrete beams, even in the case of reinforcement with stirrups, because most of the load was carried by the concrete, which is considered a brittle material that behaves linearly until failure. The yield point of beams reinforced with steel or glass mesh was challenging to see in the shear test, and it was set for all of these beams in Table.12 as a ratio of 75% ultimate load [44].

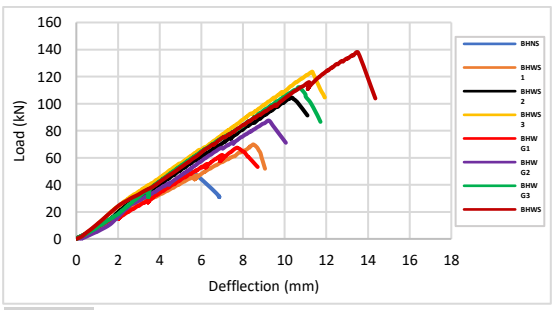

Fig. 10 Load-deflection relationships for shear beams.

Table.12 Results of the shear beam reinforced by glass and steel mesh.

Sample	First crack load Pcr (kN)	Yield load Py (kN)	Ultimate load Pu (kN)	Deflection at first crack load Δcr (mm)	Deflection at yield load Δy (mm)	Deflection at ultimate load Δu (mm)	Ductility μ	Toughness (kN.mm)
BHNS	23	37.85	50.46	2.44	4.2	5.47	1.24	137.95
BHWS	70	103.32	137.76	6.7	10	13.52	1.91	962.51
BHWS1	35	52.32	69.76	4.33	6.4	8.5	1.79	364.44
BHWS2	51	78.56	104.75	5	7.7	10.25	1.81	531.41
BHWS3	63	92.77	123.69	5.53	8.3	11.32	1.83	716.39
BHWG1	33	50.61	67.48	3.9	5.7	7.71	1.76	257.34
BHWG2	43	65.59	87.45	4.6	6.75	9.2	1.77	393.73
BHWG3	55	84.07	112.09	5.11	8	10.7	1.78	601.35

3.2. Shear ductility of ferrocement shear beams

Shear ductility is the element's ability to withstand load after the onset of a yield limit in the shear reinforcement area. To determine the shear ductility of a beam with shear reinforcement, the shear ductility index was determined by dividing the region underneath the load-deflection curve up to the ultimate shear load (Au) by the area under the curve up to the first yield of the transverse reinforcement (Ay) [45,46]:

$$\text{Ductility } (\mu) = \frac{Au}{Ay} \qquad \textbf{(1)}$$

where (μ) = shear ductility, (Au) = total energy up to the ultimate load (E_{total}), and (Ay) = the energy up to 75% of the ultimate load ($E_{@0.75Pu}$), as shown in Fig.11 [44]. By using this definition, the shear ductility was estimated from the findings of the beams in Fig.10 that had shear reinforcement. The ductility of ferrocement beams is shown in Table.13. As indicated in Fig.12, the shear ductility of the beams reinforced using layers of glass mesh was lower than those reinforced using several steel wire meshes. The ductility of the beams reinforced with fiberglass mesh (BHWG1, BHWG2, BHWG3) that have shear reinforcement ratios (0.119, 0.239, 0.359)%, respectively, was decreased by (1.68%, 2.11%, 2.68%) compared to beams reinforced with layers of steel wire mesh (BHWS1, BHWS2, BHWS3) that have shear reinforcement ratio (0.104, 0.209, 0.314)%, respectively. The reduction in ductility was a result of these brittle materials. However, the ductility of these beams increased by (41.94%, 42.89%, and 43.63%), respectively, compared to the beams that were unreinforced to shear (BHNS). Also, the ductility of the beams reinforced with layers of welded wire mesh (BHWS1, BHWS2, BHWS3) was increased by (44.66%, 45.66%, and 47.94%), respectively, compared to the beams that were unreinforced to shear (BHNS). This ductility improvement resulted from reinforcing these beams using glass or steel meshes. Despite the evident preference for ferrocement reinforced using steel meshes, the ductility increased with the number of wire meshes for both steel and glass mesh reinforcements. This result agrees with the results reported by Shaheen et al. [14], Shaheen et al. [47], and El-Sayed [18]. In these reinforced beams, the layers of steel mesh had greater ductility than the layers of glass mesh [48]. The beams reinforced with both 2 and 3 layers of steel meshes (BHWS2, BHWS3) ductility was enhanced by (0.90%) and (2.48%), respectively, compared to the beam (BHWS1). The ductility increased by (0.67% and 1.19%) for the hollow beams reinforced with 2 and 3 layers of glass meshes (BHWG2 and BHWG3), respectively, compared to (BHWG1). All the hollow beams reinforced using steel mesh or glass mesh (BHWS1, BHWS2, BHWS3, BHWG1, BHWG2, BHWG3) were reduced in ductility by (44.66%, 45.66%, 47.94%, 41.94%, 42.89%, and 43.63%), respectively, compared to beam BHWS. The reduction was obtained because the reinforcement in this beam was only steel bars and not mesh with a shear reinforcement ratio of 0.3%.

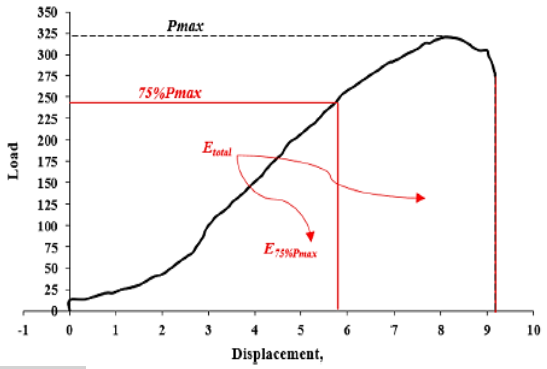

Fig. 11 Ductility energy index by Elsayed et al.[44], Alghazali et al.[46] and Hason et al.[44]

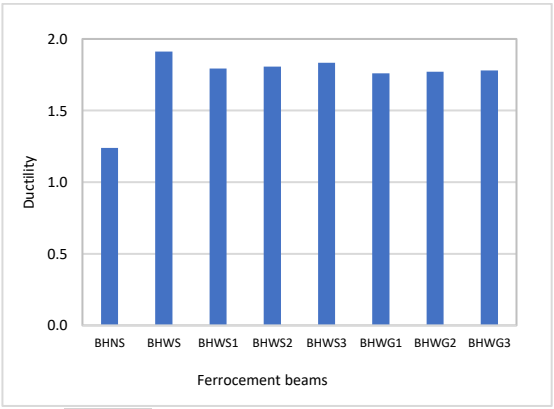

Fig. 12 Shear ductility of the beams.

Table.13 The ductility of the shear hollow ferrocement beams.

Beams	E_{total} (kN.mm)	$E_{@0.75Pu}$ (kN.mm)	Ductility (μ)
BHNS	137.95	110.92	1.24
BHWS	962.51	503.32	1.91
BHWS1	364.44	203.16	1.79
BHWS2	531.41	294.22	1.81
BHWS3	716.39	390.52	1.83
BHWG1	257.34	145.62	1.76
BHWG2	393.73	222.22	1.77
BHWG3	601.35	337.65	1.78

3.3. Toughness

Toughness is characterized as that of absorption energy needed to fracture the specimen. Toughness represents the region under the load-deflection curve; it can be determined up to the ultimate load. The shear beams' toughness energy is shown in Fig.13. Table.12 shows that the toughness of ferrocement reinforced using fiberglass mesh was less than that of ferrocement reinforced using welded meshes. The toughness energy of the ferrocement reinforced using glass mesh (BHWG1, BHWG2, BHWG3) was reduced by (29.39%, 25.91%, and 16.06%), respectively, compared with ferrocement that were reinforced using steel mesh (BHWS1, BHWS2, BHWS3). However, the toughness of these beams (BHWS1, BHWS2, BHWS3, BHWG1, BHWG2, BHWG3) was increased by (164.19%, 285.22%, 419.31%, 86.55%, 185.42%, 335.92%), respectively, compared to the beams that were unreinforced to shear (BHNS). This increase in toughness was attributed to reinforcing these beams with a fiberglass or steel mesh. The study showed that increasing the number of meshes in the ferrocement beams increased the toughness. It is in agreement with the results obtained by Shaheen et al. [49], Shaaban et al. [50], Erfan et al. [48], and El-Sayed [18]. The ultimate energy of the beams reinforced with 2 and 3 layers of steel meshes (BHWS2, BHWS3) was enhanced by about (45.81% and 96.57%), respectively, compared with the ferrocement beam (BHWS1). The ultimate energy of the beams reinforced with two and three layers of glass meshes (BHWG2, BHWG3) enhanced toughness by about (53% and 133.68%), respectively, compared to beam (BHWG1). All ferrocement reinforced using steel or glass mesh (BHWS1, BHWS2, BHWS3, BHWG1, BHWG2, BHWG3) were reduced in the ultimate energy by (62.14%, 44.79%, 25.57%, 73.26%, 59.09%, 37.52%), respectively, compared to beam BHWS because of the reinforced in this beam was steel bars not mesh. Therefore, the ultimate energy increased in this beam.

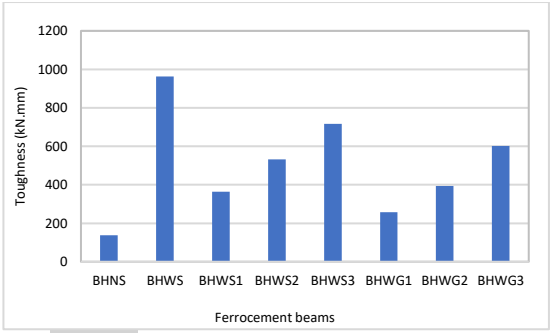

Fig. 13 Toughness of the shear beams.

3.4. Load-crack width curves and failure mechanism

Fig. 14 shows the load-crack width relationship of the ferrocement shear beams. Fig.9 shows the crack patterns of the ferrocement shear beams reinforced with fiberglass mesh and steel wire mesh. The first crack in these hollow beams was an inclined horizontal crack developed from support to upward the point load. This crack was developed in width by increasing the applied load on the beams. For beams reinforced with layers of fiberglass (BHWG1, BHWG2, BHWG3), the crack width was (1.6, 1.15, 0.85) mm, respectively, at the ultimate load that presented the largest load. The angle of failure diagonal shear cracks for these beams ranged between 41° and 44°. In contrasat, the crack width was (1.25, 1.05, and 0.9) mm, respectively, at ultimate load for beams reinforced with steel wire mesh (BHWS1, BHWS2, BHWS3). The angle of failure diagonal shear cracks for these beams ranged between 37° and 43°. The crack angle and width were smaller in steel wire mesh beams than in beams with fiberglass mesh beams. Using steel wire and fiberglass wire meshed instead of stirrups improved the crack pattern for hollow section beams, as shown in Fig.9. This can be attributed to the higher reinforcement in the form of mesh layers in the ferrocement beams and distribution cracks along the beam which, in turn, controlled crack widths. This finding is consistent with the findings of El-Sayed and Erfan [51], El-Sayed [18], and Shaaban [11], who found that the crack widths in ferrocement were smaller than those in the beams reinforced only using reinforcing rebars. The crack width was 2.1 mm of the ferrocement (BHWS) reinforced using stirrups of steel bars, not mesh. The maximum crack width was 2.65 mm for the beam (BHNS) without reinforced shear. It was observed that the crack width of the beam with stirrups was less than that of the beam without stirrups since the presence of stirrups inhibited the progression of diagonal cracks and prevented the development of shear cracking. All test beams with steel wire mesh, fiberglass mesh, stirrups, or without shear reinforcement failed in the typical shear failure mechanism with a sudden collapse. The beams with layers of

fiberglass mesh displayed brittle, diagonally typical failure collapse. The failure in these beams resulted from increasing the load, which caused the development of a diagonal crack.

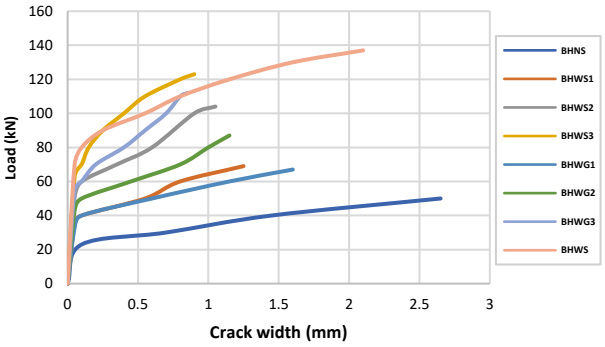

Fig. 14 Load-crack width relationship for shear beams.

4. CONCLUSIONS

Based on the results presented in the present paper, The following conclusions can be drawn:

1-The ultimate load of ferrocement reinforced with (1, 2, and 3) layers of fiberglass meshes was reduced by (3.27 %, 16.52%, and 9.38%), respectively, compared to ferrocement reinforced using meshes of welded steel (1, 2 and 3). However, compared to ferrocement that was unreinforced to shear, the ultimate load of this ferrocement was increased by 33.71%, 73.28%, and 122.11 %, respectively. In addition, the ultimate load of ferrocement reinforced using layers of welded mesh was increased by (38.23%, 107.56%, and 145.09%), respectively, compared to ferrocement that was unreinforced to resist shear with mortar only.

2-The ductility and toughness energy of the beams reinforced using several meshes of glass (1, 2, and 3) were decreased by about (1.68%, 2.11%, 2.68%) and (29.39%, 25.91%, 16.06%), respectively, when compared with beams reinforced using several welded wire steel mesh (1, 2 and 3).

3-The ultimate deflection of all ferrocement beams reinforced using glass mesh was slightly less than that of ferrocement reinforced using steel mesh. In addition, the first crack loads of all ferrocement beams reinforced using fiberglass mesh were less than ferrocement reinforced using welded mesh.

4-Using steel mesh and fiberglass mesh instead of steel stirrups reduced crack propagation, as well as the number and width of cracks decrease, particularly in ferrocement beams reinforced using two and three layers of mesh.

5-Glass and steel meshes revealed benefits over conventional reinforcement using reinforcing steel, particularly in hollow beams, such as high strength, the ability to be easily handled, cut, and molded, and low weight compared to steel stirrups.

REFERENCES

[1] Al-Kubaisy MA, Jumaat MZ. **Flexural behaviour of reinforced concrete slabs with ferrocement tension zone cover**. *Construction and Building Materials*, 2000; **14**(5): 245–252.

[2] Aboul-Anen B, El-Shafey A, El-Shami M. **Experimental and analytical model of ferrocement slabs**. *International Journal of Recent Trends in Engineering*, 2009; **1**(6): 25.

[3] Kaish A, Alam MR, Jamil M, Zain MFM, Wahed MA. **Improved ferrocement jacketing for restrengthening of square RC short column**. *Construction and Building Materials*, 2012; 36228–237.

[4] Mourad SM, Shannag MJ. **Repair and strengthening of reinforced concrete square columns using ferrocement jackets**. *Cement and concrete composites*, 2012; **34**(2): 288–294.

[5] Xiong GJ, Wu XY, Li FF, Yan Z. **Load carrying capacity and ductility of circular concrete columns confined by ferrocement including steel bars**. *Construction and Building Materials*, 2011; **25**(5): 2263–2268.

[6] Dai L, Bian H, Wang L, Potier-Ferry M, Zhang J. **Prestress loss diagnostics in pretensioned concrete structures with corrosive cracking**. *Journal of Structural Engineering*, 2020; **146**(3): 04020013.

[7] Wang L, Dai L, Bian H, Ma Y, Zhang J. **Concrete cracking prediction under combined prestress and strand corrosion**. *Structure and Infrastructure Engineering*, 2019; **15**(3): 285–295.

[8] Murthy AR, Pukazhendhi DM, Vishnuvardhan S, Saravanan M, Gandhi P. **Performance of concrete beams reinforced with GFRP bars under monotonic loading**. *Structures*, 2020; 271274–1288.

[9] Alsayed SH, Alhozaimy AM. **Ductility of concrete beams reinforced with FRP bars and steel fibers**. *Journal of composite materials*, 1999; **33**(19): 1792–1806.

[10] Daniel JI, Shah SP. Fiber reinforced concrete: developments and innovations. 1994.

[11] Shaaban IG. Expanded wire fabric permanent formwork for improving flexural behaviour of reinforced concrete beams. *Composite Materials in Concrete Construction: Proceedings of the International Seminar Held at the University of Dundee, Scotland, UK on 5–6 September* 2002; 59–70.

[12] Qu W, Zhang X, Huang H. **Flexural behavior of concrete beams reinforced with hybrid (GFRP and steel) bars**. *Journal of Composites for Construction*, 2009; **13**(5): 350–359.

[13] Li VC, Wang S. **Flexural behaviors of glass fiber-reinforced polymer (GFRP) reinforced engineered cementitious composite beams**. *Materials Journal*, 2002; **99**(1): 11–21.

[14] Shaheen YBI, Soliman NM, Hafiz AM. **Structural Behaviour of Ferrocement channels beams**. *Concrete Research Letters*, 2013; 4(3): 621–638.

[15] Erfan AM, El-Sayed TA. **Structural shear behavior of composite box beams using advanced innovated materials**. *Journal of Engineering Research and Reports*, 2019; 51–14.

[16] Erfan AM, El-Sayed TA. **Shear strength of ferrocement composite box section concrete beams**. *International Journal of Scientific & Engineering Research*, 2019; 10260–279.

[17] Abdallah AH, Erfan AM, El-Sayed TA, Abd El-Naby RM. **Experimental and analytical analysis of lightweight ferrocement composite slabs**. *Engineering Research Journal*, 2019; **1**(41): 73–85.

[18] El-Sayed TA. **Axial compression behavior of ferrocement geopolymer hsc columns**. *Polymers (Basel)*, 2021; **13**(21): 3789.

[19] Khalil AA, el Shafiey TF, Mahmoud MH, Baraghith AT, Etman AE. Shear behavior of innovated composite hollow core slabs. *International Conference on Advances in Structural and Geotechnical Engineering*, 2019.

[20] Lee C-H, Mansouri I, Kim E, Ryu J, Woo W-T. **Experimental analysis of one-way composite steel deck slabs voided by circular paper tubes: Shear strength and moment–shear interaction**. *Engineering Structures*, 2019; 182:227–240.

[21] Lee C-H, Mansouri I, Kim E, Hwang K-S, Woo W-T. **Flexural strength of one-way composite steel deck slabs voided by circular paper tubes**. *Journal of Structural Engineering*, 2019; **145**(2): 04018246.

[22] Wariyatno NG, Haryanto Y, Sudibyo GH. **Flexural behavior of precast hollow core slab using PVC pipe and Styrofoam with different reinforcement**. *Procedia Eng*, 2017; 171:909–916.

[23] Rajeshwaran R, Yamini V, Nivedha DGS, Madhu Bala AM. **Experimental evaluation of concrete slab using hollow steel pipes**. *Civil Engineering Research Journal*, 2018; **5**(4): 161–164.

[24] Abdullah AI, Ahmad SH. **Production Hollow Ferrocement Beams Through Solid Waste Recycling**. *Tikrit Journal of Engineering Sciences*, 2016; **23**(4): 11–22.

[25] Chkheiwer AH, Al-Mazini MA, Zewair MS. **Shear Behavior of Slender Ferrocement Box Beams**. *Muthanna Journal of Engineering And Technology*, 2016; 41–10.

[26] Iraqi Standard No. 5. Portland Cement. *Central Organization for Standardization and Quality Control, Baghdad, P8* 1984.

[27] Iraqi Standard Specification No.45. for Aggregate form Natural Sources for Concrete and Building Construction. *Central Organization for Standardization and Quality Control, Baghdad, Iraq, P11* 1984.

[28] Ghareeb KS, Ahmed HE, El-Affandy TH, Deifalla AF, El-Sayed TA. **The Novelty of Using Glass Powder and Lime Powder for Producing UHPSCC**. *Buildings*, 2022; **12**(5): 684.

[29] ASTM C494/C494M – 16. Standard Specification for Chemical Admixtures for Concrete. *American Society for Testing and Materials*, 2016.

[30] ASTM A615M-16. Standard Specification for Deformed and Plain Carbon-Steel Bars for Concrete Reinforcement. *American Society for Testing and Materials*, 2016.

[31] ASTM A1064M -18. Standard specification for carbon-steel wire and welded wire reinforcement, plain and deformed, for Concrete. *American Society for Testing and Materials*, 2018.

[32] EFNARC-05. Specification and Guidelines for Self-Compacting Concrete. *Surrey, UK: European Federation of National Associations Representing for Concrete* 2005; .

[33] Libre NA, Khoshnazar R, Shekarchi M. **Relationship between fluidity and stability of self-consolidating mortar incorporating chemical and mineral admixtures**. *Construction and Building Materials*, 2010; **24**(7): 1262–1271.

[34] Mehdipour I, Razzaghi MS, Amini K, Shekarchi M. **Effect of mineral admixtures on fluidity and stability of self-consolidating mortar subjected to prolonged mixing time**. *Construction and Building Materials*, 2013; 40:1029–1037.

[35] Mahdikhani M, Ramezanianpour AA. **New methods development for evaluation rheological properties of self-consolidating mortars**. *Constr Build Mater*, 2015; 75:136–143.

[36] Yaseri S, Mahdikhani M, Jafarinoor A, Verki VM, Esfandyari M, Ghiasian SM. **The development of new empirical apparatuses for evaluation fresh properties of self-consolidating mortar: Theoretical and experimental study**. *Construction and Building Materials*, 2018; 167:631–648.

[37] ASTM C109-04. Standard Test Method for Compressive Strength of Hydraulic Cement Mortars . *American Society for Testing and Materials*, 2004.

[38] ASTM C348-04. Standard Test Method for Flexural Strength of Hydraulic Cement

Mortars. *American Society for Testing and Materials,* 2004.

[39] ASTM C496-04. Standard Test Method for Splitting Tensile of Cylindrical Concrete Specimens. *American Society for Testing and Materials*, 2004.

[40] Shaaban IG, Shaheen YB, Elsayed EL, Kamal OA, Adesina PA. **Flexural characteristics of lightweight ferrocement beams with various types of core materials and mesh reinforcement**. *Construction and Building Materials,* 2018; 171:802–816.

[41] AlAli SSH, Abdulrahman MB, Tayeh BA. **Response of Reinforced Concrete Tapered Beams Strengthened Using NSM-CFRP Laminates**. *Tikrit Journal of Engineering Sciences,* 2022; **29**(1): 99–110.

[42] Ibraheem OF, Abdullah HA. **Behavior of Steel Beams Subjected to Bending and Shear Loading Under Localized Fire Conditions**. *Tikrit Journal of Engineering Sciences,* 2022; **29**(3): 82–90.

[43] Abdullah QN, Abdulla AI. **Flexural Behavior of Hollow Self Compacted Mortar Ferrocement Beam Reinforced by GFRP bars**. *Case Studies in Construction Materials,* 2022; e01556.

[44] Hason MM, Hanoon AN, Saleem SJ, Hejazi F, al Zand AW. **Characteristics of experimental ductility energy index of hybrid-CFRP reinforced concrete deep beams**. *SN Applied Sciences,* 2021; **3**(2): 1–14.

[45] Elsayed M, Tayeh BA, Aisheh YIA, Abd El-Nasser N, Abou Elmaaty M. **Shear strength of eco-friendly self-compacting concrete beams containing ground granulated blast furnace slag and fly ash as cement replacement**. *Case Studies in Construction Materials,* 2022; 17e01354.

[46] Alghazali HH, Myers JJ. **Shear behavior of full-scale high volume fly ash-self consolidating concrete (HVFA-SCC) beams**. *Constr Build Mater,* 2017; 157161–171.

[47] Shaheen YBI, Eltaly B, Abdul-Fataha S. **Structural performance of ferrocement beams reinforced with composite materials**. *Structural Engineering and Mechanics,* 2014; **50**(6): 817–834.

[48] Erfan AM, Abd Elnaby RM, Elhawary A, El-Sayed TA. **Improving the compressive behavior of RC walls reinforced with ferrocement composites under centric and eccentric loading**. *Case Studies in Construction Materials*, 2021; 14e00541.

[49] Shaheen YBI, Eltehawy EA. **Structural behaviour of ferrocement channels slabs for low cost housing**. *Challenge Journal of Concrete Research Letters,* 2017; **8**(2): 48–64.

[50] Shaaban IG, Shaheen YBI, Elsayed EL, Kamal OA, Adesina PA. **Flexural behaviour and theoretical prediction of lightweight ferrocement composite beams**. *Case Studies in Construction Materials,* 2018; 9e00204.

[51] El-Sayed TA, Erfan AM. **Improving shear strength of beams using ferrocement composite**. *Construction and Building Materials,* 2018; 172:608–617.